Critically evaluated theoretical energies, lifetimes, hyperfine constants, and multipole polarizabilities in ^{87}Rb

M. S. Safronova[1] and U. I. Safronova[2]
[1]*Department of Physics and Astronomy, 217 Sharp Lab, University of Delaware, Newark, Delaware 19716, USA*
[2]*Physics Department, University of Nevada, Reno, Nevada 89557, USA*
(Received 9 March 2011; published 18 May 2011)

Systematic study of Rb atomic properties is carried out using a high-precision relativistic all-order method. Excitation energies of the ns, np, nd, and nf ($n \leqslant 10$) states in neutral rubidium are evaluated. Reduced matrix elements, oscillator strengths, transition rates, and lifetimes are determined for the levels up to $n = 8$. Recommended values and estimates of their uncertainties are provided for a large number of electric-dipole transitions. Electric-dipole ($5s$–np, $n = 5$–26), electric-quadrupole ($5s$–nd_j, $n = 4$–26), and electric-octupole ($5s$–nf_j, $n = 4$–26) matrix elements are calculated to obtain the ground state $E1$, $E2$, and $E3$ static polarizabilities. Scalar polarizabilities of the ns, np, and nd states, and tensor polarizabilities of the $np_{3/2}$ and nd excited states of Rb are evaluated. The hyperfine A and B values in ^{87}Rb are determined for the first low-lying levels up to $n = 9$. These calculations provide recommended values critically evaluated for their accuracy for a number of Rb atomic properties useful for a variety of applications.

DOI: 10.1103/PhysRevA.83.052508 PACS number(s): 31.15.ac, 31.15.ap, 31.15.ag, 31.15.aj

I. INTRODUCTION

Accurate values of Rb atomic properties are of significant present interest owing to the importance of this system for ultracold atom studies [1–4]. For example, deterministic entanglement of two individually addressed Rb neutral atoms using a Rydberg blockade-mediated controlled-NOT gate was recently demonstrated in [2]. Rb has been recently used in mixed-species experiments with degenerate quantum gases [4]. Microwave transition between two ground-hyperfine states of ^{87}Rb was recommended as a secondary standard of a second [5]. While neutral Rb has been a subject of a number of experimental studies, a large fraction of them focused on the first few lowest levels. Very few theoretical data have been evaluated for their accuracy. In this work, we carry out extensive study of Rb properties using the all-order method and evaluate the accuracy of our results. In particular, recommended values of polarizabilities for a number of excited states are given. Importance of the polarizabilities for a variety of applications was recently discussed in the review [6]. We note that Rb represents an excellent benchmark case for the theory vs experiment comparisons owing to its relatively simple electronic structure and well-developed experimental techniques. Several high-precision measurements of Rb properties have been conducted recently [7–11] and present another motivation for this work. The availability of high-precision predictions may be not only useful for a variety of current experiments, but also may stimulate further experimental work in benchmark high-precision measurements. We give a brief overview of the earlier experimental and theoretical studies of Rb properties below.

Energies, oscillator strengths, radiative transition rates, and lifetimes in Rb have been studied experimentally and theoretically in Refs. [8,11–32] during the past few decades. A large number of publications were also devoted to other properties such as multipole polarizabilities [33–40] and hyperfine constants [9,10,41–50].

Recently, the lifetimes of the $6s$ and $5d$ states of rubidium have been measured with high precision in Refs. [8,11]. Polarizabilities of highly excited rubidium $9s$, $10s$, and $8d_j$ states were determined by measuring the stark shifts of transitions using an electro-optically modulated laser beam to excite an atomic beam [7]. The scalar α_0 and tensor α_2 polarizability values were 100 times more accurate than previous measurements [36,37]. Such high accuracy of experimental measurements is a challenge for tests of high-precision approaches and is one of the motivating factors for this work.

The compilation of experimental measurements of hyperfine magnetic-dipole (A) and electric-quadrupole (B) constants in ^{85}Rb and ^{87}Rb was presented by Arimondo *et al.* [45]. In that review, all measurements carried out before 1977 were included. More recent measurements of the A and B hyperfine constants of the $6d_{3/2}$, $7d_{3/2}$, and $8d_{3/2}$ states in ^{85}Rb were published by Van Wijngaarden *et al.* [46–48]. Quantum beats due to the hyperfine interaction were observed in the radiative decay of the $6d_{3/2}$, $7d_{3/2}$, and $8d_{3/2}$ states in Rb. The quantum beat technique has the advantage of not needing any external magnetic fields [46–48]. The only restriction on the quantum beat method is the requirement that the hyperfine coupling times be less than the excited-state lifetime and greater than the excitation pulse duration [46–48]. Using laser-cooled samples of ^{85}Rb and ^{87}Rb in a magneto-optical trap and high-resolution spectroscopy, the two-photon transitions $5s$–$5d_{3/2}$, $5s$–$5d_{5/2}$, and $5s$–$7s$ were investigated by Snadden *et al.* [49] using the output from a mode-locked titanium sapphire laser. The hyperfine constants for the $7s$ term of both isotopes have been measured with improved accuracy in comparison with results in [45]. The absolute frequencies of the rubidium $5s$–$7s$ two-photon transition at 760 nm were measured recently [9] to an accuracy of 20 kHz with an optical frequency comb based on a mode-locked femtosecond Ti:sapphire laser. The accuracy of the hyperfine constant of the $7s$ state was improved in Ref. [9] by a factor of 5 in comparison with previous result [49]. A hyperfine anomaly in the measurement of the hyperfine

splitting of the $6s$ excited level in ^{87}Rb was observed in [10]. This measurement was performed by a two-step spectroscopy using the $5s$–$5p_{1/2}$–$6s$ excitation sequence. The splitting of the $6s$ level was measured to obtain the magnetic dipole constants with a high level of accuracy [10].

One of the first high-precision *ab initio* calculations of Rb atomic properties was presented by Johnson *et al.* [51] using third-order perturbation theory with the additional estimates of selected higher-order terms. The amplitudes of the $5p_j \rightarrow 5s$ and the $6s \rightarrow 5p_j$ transitions in Rb and similar transitions in other alkali-metal atoms were evaluated [51]. Ground- and excited-state energies, ionization potentials, and electron affinities were calculated for all the alkali-metal atoms using the relativistic Fock-space single-double coupled-cluster (CCSD) method in Ref. [52]. High-accuracy calculation of the removal energies of Rb, Cs, Fr, and element 119 was carried out in Ref. [53] using the CCSD method starting from the Dirac-Coulomb-Breit Hamiltonian. The relativistic many-body calculations of atomic properties for alkali-metal atoms were presented by Safronova *et al.* [54–58]. Those calculations were carried out using the relativistic single-double (SD) method in which single and double excitations of Dirac-Fock wave functions are included to all orders of perturbation theory and provided accurate values of removal energies, electric-dipole matrix elements, hyperfine constants, and static polarizabilities [54–58]. Determination of electric-dipole matrix elements in K and Rb from Stark shift measurements was carried out in [58]. Magic wavelengths for the ns–np transitions in alkali-metal atoms were calculated in [57]. Blackbody radiation shift in ^{87}Rb microwave frequency standard was calculated with 0.3% accuracy in [59]. A state-insensitive bichromatic optical trapping scheme was studied on the example of Rb in Ref. [60].

In the present paper, the relativistic all-order method is used to calculate atomic properties of neutral rubidium for the ns, np_j, nd_j, and nf_j ($n \leqslant 12$) states. We evaluate a large number of transition matrix elements to calculate $E1$, $E2$, and $E3$ ground-state polarizabilities, scalar polarizabilities of the ns, np, and nd states, and tensor polarizabilities of the $np_{3/2}$ and nd excited states of Rb. Excitation energies are calculated for the 41 first excited states. The hyperfine A and B values are determined for the first low-lying levels up to $n = 9$. The main motivation for this work is to provide recommended values for a number of atomic properties via a systematic high-precision study for use in planning and analysis of various experiments as well as theoretical modeling.

II. THIRD-ORDER AND ALL-ORDER CALCULATIONS OF ENERGIES

Energies of nl_j states in Rb were evaluated for $n \leqslant 10$ and $l \leqslant 3$ using both third-order relativistic many-body perturbation theory (RMBPT) and the SD all-order method discussed in Ref. [61], in which single and double excitations of Dirac-Fock (DF) wave functions are iterated to all orders. Performing both calculations makes it possible to evaluate the effects of the fourth and higher orders. We use very large $N = 70$ B-spline basis set [62] to increase the number of states that can be considered. The present calculation of the polarizabilities required accurate representation of rather highly excited states, such as $6l$–$13l$, leading to the use of the large $R = 220$ a.u. cavity for the generation of the finite basis set. As a result, a higher number of basis states was required to produce high-accuracy single-particle orbitals. Results of our energy calculations are summarized in Table I. Columns 2–8 of Table I give the lowest-order DF energies $E^{(0)}$, second-order and third-order Coulomb correlation energies $E^{(2)}$ and $E^{(3)}$, first-order and second-order Breit corrections $B^{(1)}$ and $B^{(2)}$, and an estimated Lamb shift contribution, $E^{(\mathrm{LS})}$. The Lamb shift $E^{(\mathrm{LS})}$ is calculated as the sum of the one-electron self-energy and the first-order vacuum-polarization energy. The vacuum-polarization contribution is calculated from the Uehling potential using the results of Fullerton and Rinker [64]. The self-energy contribution is estimated for the s and p orbitals by interpolating among the values obtained by Mohr [65–67] using Coulomb wave functions. We note that the $E^{(\mathrm{LS})}$ is above 0.1 cm^{-1} only for the ground state.

We list the all-order SD energies in the column labeled E^{SD} and list the part of the third-order energy missing from E^{SD} in the column labeled $E^{(3)}_{\mathrm{extra}}$. The sum of the six terms $E^{(0)}$, E^{SD}, $E^{(3)}_{\mathrm{extra}}$, $B^{(1)}$, $B^{(2)}$, and $E^{(\mathrm{LS})}$ is our final all-order result $E^{\mathrm{SD}}_{\mathrm{tot}}$, listed in the 11th column of Table I. Recommended energies from the National Institute of Standards and Technology (NIST) database [63] are given in the column labeled E_{NIST}. Differences between our third-order and all-order calculations and experimental data, $\delta E^{(3)} = E^{(3)}_{\mathrm{tot}} - E_{\mathrm{NIST}}$ and $\delta E^{\mathrm{SD}} = E^{\mathrm{SD}}_{\mathrm{tot}} - E_{\mathrm{NIST}}$, are given in the two final columns of Table I, respectively.

As expected, the largest correlation contribution to the valence energy comes from the second-order term $E^{(2)}$. Therefore, we calculate $E^{(2)}$ with higher numerical accuracy. The second-order energy includes partial waves up to $l_{\max} = 8$ and is extrapolated to account for contributions from higher partial waves (see, for example, Refs. [68,69] for details of the extrapolation procedure). As an example of the convergence of $E^{(2)}$ with the number of partial waves l, consider the $5s$ state. Calculations of $E^{(2)}$ with $l_{\max} = 6$ and 8 yield $E^{(2)}(5s) = -3283.1$ and -3297.8 cm^{-1}, respectively. Extrapolation of these calculations yields -3306.1 and -3306.8 cm^{-1}, respectively, resulting in numerical uncertainty in $E^{(2)}(5s)$ of 0.7 cm^{-1}. Smaller (about 4–6 cm^{-1}) contributions are obtained for the $4d$, $5p$, and $5d$ states and much smaller contributions (0.5–1.5 cm^{-1}) are obtained for the $n = 6$ states.

Owing to the numerical complexity, we restrict $l \leqslant l_{\max} = 6$ in the E^{SD} calculation. As noted above, the second-order contribution dominates E^{SD}; therefore, we can use the extrapolated value of the $E^{(2)}$ described above to account for the contributions of the higher partial waves. Six partial waves are also used in the calculation of $E^{(3)}$.

The column labeled δE^{SD} in Table I gives differences between our *ab initio* results and the experimental values [63]. The SD results agree better with the measured values than do the third-order MBPT results (the ratio of $\delta E^{(3)}/\delta E^{\mathrm{SD}}$ is about 10 for some cases), illustrating the importance of fourth and higher-order correlation corrections. The all-order values are in excellent agreement with experiment.

TABLE I. Zeroth-order (DF), second-order, and third-order Coulomb correlation energies $E^{(n)}$, single-double Coulomb energies $E^{\rm SD}$, $E^{(3)}_{\rm extra}$, first-order Breit and second-order Coulomb-Breit corrections $B^{(n)}$ to the energies of Rb. The total energies ($E^{(3)}_{\rm tot} = E^{(0)} + E^{(2)} + E^{(3)} + B^{(1)} + B^{(2)}$, $E^{\rm SD}_{\rm tot} = E^{(0)} + E^{\rm SD} + E^{(3)}_{\rm extra} + B^{(1)} + B^{(2)}$) are compared with experimental values $E_{\rm NIST}$ [63], $\delta E = E_{\rm tot} - E_{\rm NIST}$. Units: cm^{-1}.

nlj	$E^{(0)}$	$E^{(2)}$	$E^{(3)}$	$B^{(1)}$	$B^{(2)}$	$E^{\rm (LS)}$	$E^{(3)}_{\rm tot}$	$E^{\rm SD}$	$E^{(3)}_{\rm extra}$	$E^{\rm SD}_{\rm tot}$	$E_{\rm NIST}$	$\delta E^{(3)}$	$\delta E^{\rm SD}$
$5s_{1/2}$	−30 571	−3306.1	678.5	19.3	−30.1	1.7	−33 208	−3448.3	364.3	−33 664	−33 691	483	27
$5p_{1/2}$	−19 932	−1196.5	202.8	9.8	−9.1	0.0	−20 925	−1308.3	124.2	−21 115	−21 112	187	−3
$5p_{3/2}$	−19 750	−1139.7	192.5	7.2	−9.3	0.0	−20 699	−1243.5	118.0	−20 877	−20 874	175	−3
$4d_{3/2}$	−13 100	−1055.2	185.7	2.5	−9.6	0.0	−13 976	−1305.2	109.2	−14 303	−14 335	359	32
$4d_{5/2}$	−13 113	−1049.2	183.2	1.9	−9.4	0.0	−13 986	−1294.2	107.9	−14 306	−14 336	350	29
$4f_{5/2}$	−6860	−38.5	4.1	0.0	0.0	0.0	−6895	−41.0	4.2	−6897	−6899	4	2
$4f_{7/2}$	−6860	−38.5	4.1	0.0	0.0	0.0	−6895	−41.0	4.2	−6897	−6899	4	2
$5d_{3/2}$	−7405	−538.3	101.0	1.6	−6.0	0.0	−7847	−627.3	55.2	−7982	−7990	143	9
$5d_{5/2}$	−7411	−532.4	99.0	1.2	−5.8	0.0	−7849	−617.9	54.2	−7980	−7987	138	8
$5f_{5/2}$	−4391	−22.2	2.4	0.0	0.0	0.0	−4411	−23.7	2.4	−4412	−4413	3	1
$5f_{7/2}$	−4391	−22.2	2.4	0.0	0.0	0.0	−4411	−23.6	2.4	−4412	−4413	3	1
$6s_{1/2}$	−12 884	−760.8	163.3	5.2	−7.8	0.0	−13 484	−731.2	84.6	−13 533	−13 557	73	25
$6p_{1/2}$	−9633	−361.6	64.8	3.4	−3.2	0.0	−9929	−375.6	37.5	−9971	−9976	46	5
$6p_{3/2}$	−9569	−346.3	61.9	2.5	−3.3	0.0	−9854	−359.6	35.8	−9894	−9898	44	5
$6d_{3/2}$	−4705	−287.6	55.1	0.9	−3.4	0.0	−4940	−320.4	29.4	−4999	−5004	63	5
$6d_{5/2}$	−4708	−283.7	53.9	0.7	−3.3	0.0	−4941	−314.7	28.7	−4997	−5001	61	4
$6f_{5/2}$	−3049	−13.6	1.5	0.0	0.0	0.0	−3061	−14.5	1.5	−3062	−3063	2	1
$6f_{7/2}$	−3049	−13.6	1.5	0.0	0.0	0.0	−3061	−14.5	1.5	−3062	−3063	2	1
$7s_{1/2}$	−7120	−298.2	65.0	2.1	−3.2	0.0	−7354	−279.9	33.2	−7368	−7379	25	12
$7p_{1/2}$	−5706	−160.3	29.2	1.6	−1.5	0.0	−5837	−163.6	16.6	−5853	−5856	19	3
$7p_{3/2}$	−5676	−153.9	28.0	1.2	−1.5	0.0	−5802	−157.1	15.9	−5818	−5821	18	3
$7d_{3/2}$	−3241	−167.9	32.5	0.6	−2.1	0.0	−3378	−181.7	17.1	−3407	−3411	32	3
$7d_{5/2}$	−3243	−165.3	31.7	0.4	−2.0	0.0	−3378	−178.2	16.7	−3406	−3409	31	3
$7f_{5/2}$	−2240	−9.0	1.0	0.0	0.0	0.0	−2248	−9.5	1.0	−2249	−2249	1	0
$7f_{7/2}$	−2240	−9.0	1.0	0.0	0.0	0.0	−2248	−9.5	1.0	−2249	−2249	1	0
$8s_{1/2}$	−4516	−147.8	32.4	1.1	−1.6	0.0	−4632	−137.3	16.5	−4638	−4644	12	6
$8p_{1/2}$	−3777	−85.3	15.7	0.9	−0.8	0.0	−3846	−86.4	8.8	−3854	−3856	10	2
$8p_{3/2}$	−3761	−82.1	15.1	0.6	−0.8	0.0	−3828	−83.1	8.5	−3835	−3837	9	2
$8d_{3/2}$	−2365	−106.4	20.7	0.4	−1.3	0.0	−2451	−112.2	10.8	−2467	−2469	18	2
$8d_{5/2}$	−2366	−104.7	20.2	0.3	−1.3	0.0	−2451	−110.0	10.6	−2466	−2468	17	2
$9s_{1/2}$	−3120	−84.1	18.5	0.6	−0.9	0.0	−3185	−77.6	9.4	−3188	−3192	6	4
$9p_{1/2}$	−2685	−50.9	9.4	0.5	−0.5	0.0	−2726	−51.2	5.3	−2731	−2732	6	1
$9p_{3/2}$	−2675	−49.0	9.0	0.4	−0.5	0.0	−2715	−49.3	5.1	−2720	−2721	5	1
$9d_{3/2}$	−1800	−70.6	13.8	0.3	−0.9	0.0	−1857	−73.9	7.2	−1867	−1869	12	2
$9d_{5/2}$	−1800	−69.5	13.4	0.2	−0.9	0.0	−1857	−72.4	7.0	−1867	−1868	11	2
$10s_{1/2}$	−2284	−52.4	11.6	0.4	−0.6	0.0	−2325	−48.1	5.8	−2326	−2328	4	2
$10p_{1/2}$	−2007	−32.8	6.1	0.3	−0.3	0.0	−2033	−32.9	3.4	−2036	−2037	3	1
$10p_{3/2}$	−2000	−31.6	5.8	0.3	−0.3	0.0	−2026	−31.7	3.3	−2029	−2030	3	1
$10d_{3/2}$	−1415	−49.4	9.7	0.2	−0.6	0.0	−1455	−51.3	5.0	−1462	−1463	8	1
$10d_{5/2}$	−1416	−48.6	9.4	0.1	−0.6	0.0	−1455	−50.2	4.9	−1461	−1463	7	1
$11s_{1/2}$	−1744	−34.9	7.7	0.3	−0.4	0.0	−1771	−31.9	3.9	−1772	−1774	2	2

III. ELECTRIC-DIPOLE MATRIX ELEMENTS, OSCILLATOR STRENGTHS, TRANSITION RATES, AND LIFETIMES

A. Electric-dipole matrix elements

In Table II, we list our recommended values for the 50 $E1$ $ns-n'p$, $nd-n'p$, and $nd-n'f$ transitions. We note that we have calculated more than 500 $E1$ matrix elements to evaluate lifetimes and polarizabilities presented in this work. We list only the matrix elements that give significant contributions to the atomic properties calculated in the other sections. To evaluate the uncertainties of these values, we carried out several calculations in different approximations. We list the lowest-order DF $Z^{\rm DF}$, second-order $Z^{\rm (DF+2)}$, and third-order $Z^{\rm (DF+2+3)}$ values in the first three numerical columns of Table II to demonstrate the size of the second-, third-, and higher-order correlation corrections. The absolute values of the reduced matrix elements in atomic units ($a_0 e$) are given in all cases. The many-body perturbation theory (MBPT) calculations are carried out following the method described in Ref. [70]. The values $Z^{\rm (DF+2)}$ are obtained as the sum of the second-order correlation correction $Z^{(2)}$ and the DF matrix elements $Z^{\rm DF}$. The third-order matrix elements $Z^{\rm (DF+2+3)}$ include the DF values, the second-order

TABLE II. Recommended values of the reduced electric-dipole matrix elements in atomic units. The first-order, second-order, third-order MBPT, and all-order SD and SDpT values are listed; the label "sc" indicates the scaled values. Final recommended values and their uncertainties are given in the $Z^{\rm final}$ column. The last column gives relative uncertainties of the final values in %. Absolute values are given.

Transition		$Z^{\rm DF}$	$Z^{\rm (DF+2)}$	$Z^{\rm (DF+2+3)}$	$Z^{\rm SD}$	$Z^{\rm (SD)}_{\rm sc}$	$Z^{\rm SDpT}$	$Z^{\rm SDpT}_{\rm sc}$	$Z^{\rm final}$	Unc. (%)
$5s_{1/2}$	$5p_{1/2}$	4.8189	4.5981	4.1855	4.2199	4.2535	4.2652	4.2498	4.253(34)	0.79
$5s_{1/2}$	$5p_{3/2}$	6.8017	6.4952	5.9047	5.9550	6.0031	6.0196	5.9976	6.003(48)	0.80
$6s_{1/2}$	$5p_{1/2}$	4.2564	4.2895	4.1873	4.1187	4.1451	4.1355	4.1391	4.145(10)	0.23
$6s_{1/2}$	$5p_{3/2}$	6.1865	6.2278	6.1121	6.0145	6.0472	6.0342	6.0385	6.047(13)	0.21
$6s_{1/2}$	$6p_{1/2}$	10.2856	10.2275	9.5916	9.6839	9.7210	9.7452	9.7133	9.721(24)	0.25
$6s_{1/2}$	$6p_{3/2}$	14.4575	14.3787	13.4581	13.5918	13.6468	13.6806	13.6356	13.647(34)	0.25
$7s_{1/2}$	$5p_{1/2}$	0.9809	0.9983	0.9506	0.9543	0.9527	0.9581	0.9576	0.953(05)	0.57
$7s_{1/2}$	$5p_{3/2}$	1.3925	1.4152	1.3457	1.3521	1.3498	1.3577	1.3567	1.350(08)	0.59
$7s_{1/2}$	$6p_{1/2}$	9.3594	9.3793	9.2898	9.1896	9.2258	9.2092	9.2149	9.226(17)	0.18
$7s_{1/2}$	$6p_{3/2}$	13.5514	13.5739	13.4980	13.3529	13.3959	13.3754	13.3813	13.396(21)	0.15
$7s_{1/2}$	$7p_{1/2}$	17.6123	17.5916	16.7074	16.8435	16.8881	16.9284	16.8751	16.888(40)	0.24
$7s_{1/2}$	$7p_{3/2}$	24.7076	24.6820	23.3878	23.5865	23.6546	23.7109	23.6361	23.655(56)	0.24
$7s_{1/2}$	$8p_{1/2}$	1.8006	1.7842	1.9447	1.8653	1.8577	1.8557	1.8761	1.858(18)	0.99
$7s_{1/2}$	$8p_{3/2}$	2.7269	2.7019	2.9432	2.8330	2.8192	2.8178	2.8444	2.819(25)	0.89
$8s_{1/2}$	$5p_{1/2}$	0.5139	0.5254	0.5012	0.5037	0.5022	0.5054	0.5048	0.502(03)	0.64
$8s_{1/2}$	$5p_{3/2}$	0.7265	0.7414	0.7056	0.7098	0.7077	0.7124	0.7114	0.708(05)	0.66
$8s_{1/2}$	$6p_{1/2}$	1.9219	1.9327	1.8390	1.8532	1.8510	1.8616	1.8597	1.851(11)	0.58
$8s_{1/2}$	$6p_{3/2}$	2.7047	2.7192	2.5776	2.6001	2.5974	2.6129	2.6098	2.597(16)	0.60
$4d_{3/2}$	$5p_{1/2}$	9.0464	8.8368	8.1134	7.9802	8.0369	7.9943	8.0150	8.037(43)	0.53
$4d_{3/2}$	$5p_{3/2}$	4.0817	3.9888	3.6644	3.6029	3.6276	3.6076	3.6177	3.628(20)	0.55
$4d_{3/2}$	$7p_{1/2}$	1.1811	1.2154	1.1181	1.0909	1.0914	1.0839	1.0881	1.091(07)	0.68
$4d_{3/2}$	$7p_{3/2}$	0.5339	0.5492	0.5016	0.4880	0.4884	0.4843	0.4870	0.488(04)	0.85
$4d_{3/2}$	$8p_{1/2}$	0.5780	0.6018	0.5667	0.5551	0.5548	0.5526	0.5529	0.555(02)	0.40
$4d_{3/2}$	$8p_{3/2}$	0.2623	0.2729	0.2552	0.2492	0.2491	0.2477	0.2483	0.249(01)	0.57
$4d_{5/2}$	$5p_{3/2}$	12.2411	11.9624	10.9928	10.8149	10.8894	10.8313	10.8600	10.889(58)	0.53
$4d_{5/2}$	$7p_{3/2}$	1.6007	1.6463	1.5033	1.4641	1.4656	1.4536	1.4617	1.466(12)	0.82
$4d_{5/2}$	$8p_{3/2}$	0.7866	0.8183	0.7649	0.7475	0.7475	0.7434	0.7452	0.748(04)	0.54
$5d_{3/2}$	$6p_{1/2}$	18.7006	18.6322	18.2462	18.1341	18.1955	18.1879	18.1627	18.195(87)	0.48
$5d_{3/2}$	$6p_{3/2}$	8.4432	8.4119	8.2347	8.1778	8.2046	8.1999	8.1905	8.205(27)	0.33
$5d_{3/2}$	$8p_{1/2}$	2.6597	2.6818	2.5717	2.4613	2.4628	2.4570	2.4675	2.463(06)	0.23
$5d_{3/2}$	$8p_{3/2}$	1.1972	1.2070	1.1461	1.0943	1.0960	1.0920	1.0982	1.096(04)	0.37
$5d_{5/2}$	$6p_{3/2}$	25.3401	25.2467	24.7022	24.5410	24.6208	24.6085	24.5791	24.621(80)	0.32
$5d_{5/2}$	$8p_{3/2}$	3.5909	3.6199	3.4343	3.2870	3.2920	3.2810	3.2987	3.292(11)	0.33
$7d_{3/2}$	$5p_{1/2}$	0.4468	0.4911	0.8134	0.8074	0.7977	0.8046	0.7899	0.798(08)	0.97
$7d_{3/2}$	$5p_{3/2}$	0.2170	0.2359	0.3831	0.3793	0.3745	0.3777	0.3711	0.374(03)	0.91
$7d_{5/2}$	$5p_{3/2}$	0.6582	0.7150	1.1441	1.1310	1.1179	1.1262	1.1082	1.118(10)	0.87
$8d_{3/2}$	$5p_{1/2}$	0.3691	0.4022	0.6341	0.6190	0.6125	0.6158	0.6081	0.613(04)	0.72
$8d_{3/2}$	$5p_{3/2}$	0.1774	0.1915	0.2970	0.2894	0.2862	0.2877	0.2843	0.286(02)	0.67
$8d_{5/2}$	$5p_{3/2}$	0.5372	0.5795	0.8865	0.8630	0.8545	0.8582	0.8490	0.855(06)	0.64
$4d_{3/2}$	$5f_{5/2}$	5.0656	5.0042	4.7764	4.5951	4.6143	4.5755	4.6031	4.614(39)	0.84
$4d_{3/2}$	$6f_{5/2}$	2.9432	2.8960	2.9284	2.8192	2.8234	2.8113	2.8146	2.823(17)	0.61
$4d_{3/2}$	$8f_{5/2}$	1.5101	1.4794	1.5657	1.5110	1.5021	1.5088	1.5051	1.502(13)	0.84
$4d_{5/2}$	$5f_{5/2}$	1.3532	1.3368	1.2758	1.2287	1.2339	1.2238	1.2309	1.234(10)	0.82
$4d_{5/2}$	$5f_{7/2}$	6.0517	5.9782	5.7055	5.4948	5.5182	5.4730	5.5050	5.518(45)	0.82
$4d_{5/2}$	$6f_{5/2}$	0.7869	0.7743	0.7823	0.7538	0.7550	0.7519	0.7527	0.755(04)	0.58
$4d_{5/2}$	$6f_{7/2}$	3.5190	3.4626	3.4985	3.3713	3.3765	3.3625	3.3663	3.377(20)	0.58
$4d_{5/2}$	$8f_{5/2}$	0.4040	0.3958	0.4183	0.4041	0.4018	0.4035	0.4025	0.402(03)	0.80
$4d_{5/2}$	$8f_{7/2}$	1.8067	1.7701	1.8708	1.8070	1.7969	1.8045	1.8002	1.797(14)	0.79
$5d_{3/2}$	$4f_{5/2}$	25.4460	25.4339	25.6456	25.3138	25.3569	25.3007	25.3164	25.357(56)	0.22
$5d_{5/2}$	$4f_{5/2}$	6.8028	6.7996	6.8537	6.7677	6.7789	6.7645	6.7681	6.779(14)	0.21
$5d_{5/2}$	$4f_{7/2}$	30.4226	30.4081	30.6505	30.2657	30.3160	30.2517	30.2679	30.316(64)	0.21

$Z^{(2)}$ results, and the third-order $Z^{(3)}$ correlation correction. $Z^{(3)}$ includes random-phase-approximation (RPA) terms iterated to all orders, Brueckner orbital (BO) corrections, the structural radiation, and the normalization terms (see [70] for definitions of these terms).

The next four columns of Table II contain four different all-order calculations. *Ab initio* electric-dipole matrix elements evaluated in the all-order SD and SDpT approximations (SD all-order method including partial triple excitations [71]) are given in columns labeled $Z^{\rm SD}$ and $Z^{\rm SDpT}$. Differences between the $Z^{\rm SD}$ and $Z^{\rm SDpT}$ values are generally 0.5%–2.0% for the transitions listed in Table II. The SD and SDpT matrix elements $Z^{\rm SD}$ include $Z^{(3)}$ completely, along with important fourth- and higher-order corrections. The fourth-order corrections omitted from the SD matrix elements were discussed by Derevianko and Emmons [72].

Recently, we developed some general criteria to establish the final values for all transitions and evaluate uncertainties owing to the need to analyze a very large number of transitions [73]. To evaluate the uncertainties of our matrix elements and to provide recommended values, we carried out semiempirical evaluation of the missing correlation corrections using the scaling procedure. The uncertainty evaluation was discussed in detail in Ref. [73], and we briefly summarize it below.

The matrix elements of any one-body operator $Z = \sum_{ij} z_{ij}\ a_i^\dagger a_j$ are obtained within the framework of the SD all-order method as

$$Z_{wv} = \frac{\langle\Psi_w|Z|\Psi_v\rangle}{\sqrt{\langle\Psi_v|\Psi_v\rangle\langle\Psi_w|\Psi_w\rangle}}. \tag{1}$$

The $|\Psi_v\rangle$ and $|\Psi_w\rangle$ are given by the expansions

$$|\Psi_v\rangle = \left[1 + \sum_{ma}\rho_{ma}a_m^\dagger a_a + \frac{1}{2}\sum_{mnab}\rho_{mnab}a_m^\dagger a_n^\dagger a_b a_a + \sum_{m\neq v}\rho_{mv}a_m^\dagger a_v + \sum_{mna}\rho_{mnva}a_m^\dagger a_n^\dagger a_a a_v\right]\left|\Psi_v^{(0)}\right\rangle, \tag{2}$$

where $|\Psi_v^{(0)}\rangle$ is the lowest-order atomic state vector. In Eq. (2), the indices m and n range over all possible virtual states while indices a and b range over all occupied core states. The quantities ρ_{ma}, ρ_{mv}, ρ_{mnab}, and ρ_{mnva} are single-excitation coefficients for core and valence electrons and double-excitation coefficients for core and valence electrons, respectively. In the SD approximation, the resulting expression for the numerator of Eq. (1) consists of the sum of the DF matrix element z_{wv} and 20 other terms that are linear or quadratic functions of the excitation coefficients.

However, only two terms give dominant contributions for all transition matrix elements considered in this work:

$$Z^{(a)} = \sum_{ma}(z_{am}\tilde{\rho}_{wmva} + z_{ma}\tilde{\rho}^*_{vmwa}) \tag{3}$$

and

$$Z^{(c)} = \sum_{m}(z_{wm}\rho_{mv} + z_{mv}\rho^*_{mw}), \tag{4}$$

where $\tilde{\rho}_{mnab} = \rho_{mnab} - \rho_{nmab}$ and z_{wv} are lowest-order matrix elements of the corresponding one-body operator. For most of the transitions considered in this work, term $Z^{(c)}$ is the dominant term. To evaluate missing corrections to this term, we need to improve the values of the valence single-excitation coefficients ρ_{mv} [74]. These excitation coefficients are closely related to the correlation energy δE_v. The omitted correlation correction can be estimated by adjusting the single-excitation coefficients ρ_{mv} to the experimentally known value of the valence correlation energy and then recalculating the matrix elements using Eq. (1) with the modified coefficients [74]

$$\rho'_{mv} = \rho_{mv}\frac{\delta E_v^{\rm expt}}{\delta E_v^{\rm theory}}. \tag{5}$$

The $\delta E_v^{\rm expt}$ is defined as the experimental energy [63] minus the lowest-order DF energy ϵ_v. This is a rather complicated procedure that involves complete recalculation of the matrix elements with new values of the valence excitation coefficients. The scaling factors depend on the correlation energy given by the particular calculation. Therefore, the scaling factors are different for the SD and SDpT calculations, and these values have to be scaled separately. The corresponding results are listed in Table II with subscript "sc". The scaled SD and SDpT values are close together, as expected.

The term $Z^{(a)}$ is not corrected by the scaling procedure. However, it is dominant for very few transitions that give significant contributions to the atomic properties considered in this work, and we consider such cases separately. Therefore, we can establish the recommended set of values and their uncertainties based on the ratio $R = Z^{(c)}/Z^{(a)}$. We take the SD scaled result as the final value if $R > 1$. Otherwise, we use the SD result as the final value. If $0.5 < R < 1.5$, we evaluate the uncertainty in term $Z^{(c)}$ as the maximum difference of the final value and the other three all-order values from the SD, SDpT, SDsc, and SDpTsc set. We assume that the uncertainty of all the other terms does not exceed this value and add two uncertainties in quadrature. If $1.5 < R < 3$, we evaluate the final uncertainty as the max(SDsc-SD, SDsc-SDpT, SDsc-SDpTsc). If the term $Z^{(c)}$ strongly dominates and $R > 3$, we evaluate the final uncertainty as max(SDsc-SDpT, SDsc-SDpTsc). In the case of the $5d-5p$ matrix elements, the uncertainty is determined as the difference of the scaled SD and SDpT data owing to very large correlation correction. We have conducted numerous comparisons of all available data on various properties of many different monovalent systems with different types of experiments in many other works (see [71,73–83] and references therein) and found that such procedures do not underestimate the uncertainties but may somewhat overestimate them in some cases. The electric-dipole matrix elements for transitions involving nd states are generally very strongly dominated by the term $Z^{(c)}$. Therefore, we carried out two sets of the SD calculations for the nd states to further evaluate the uncertainty and stability of the scaling procedure. In the first run, we allow the valence excitation coefficients to converge to a specified numerical criteria; that is, the iteration process terminates when the relative difference between valence correlations energies resulting from two subsequent iterations is below 0.0001. In the second run, we terminate the iteration process after the third iteration, which results in the scaling factor near 1, closely reproducing the experimental correlation energy. Scaling was carried out in both cases and the consistency of

TABLE III. Wavelengths λ (Å), transition rates A (s^{-1}) and oscillator strengths f for transitions in Rb calculated using our recommended values of reduced electric-dipole matrix elements $Z^{\rm final}$ and their uncertainties. The relative uncertainties in the values of transition rates and oscillator strengths are the same. They are listed in column "Unc." in %. Numbers in brackets represent powers of 10.

Transition		λ	A	f	Unc.(%)	Transition		λ	A	f	Unc.(%)
$5s_{1/2}$	$5p_{1/2}$	7949.8	3.648[7]	3.456[−1]	1.58	$5p_{3/2}$	$8d_{3/2}$	5433.3	2.587[5]	1.145[−3]	1.34
$5s_{1/2}$	$5p_{3/2}$	7802.4	3.843[7]	7.015[−1]	1.60	$5p_{3/2}$	$8d_{5/2}$	5433.0	1.537[6]	1.021[−2]	1.28
$6s_{1/2}$	$6p_{1/2}$	27 912.9	4.402[6]	5.142[−1]	0.50	$6p_{1/2}$	$5d_{3/2}$	50 366.3	1.313[6]	9.983[−1]	0.96
$6s_{1/2}$	$6p_{3/2}$	27 321.8	4.625[6]	1.035[0]	0.50	$6p_{3/2}$	$5d_{3/2}$	52 412.4	2.368[5]	9.753[−2]	0.66
$7s_{1/2}$	$7p_{1/2}$	65 634.8	1.022[6]	6.600[−1]	0.48	$6p_{3/2}$	$5d_{5/2}$	52 331.2	1.428[6]	8.796[−1]	0.64
$7s_{1/2}$	$7p_{3/2}$	64 157.1	1.073[6]	1.325[0]	0.48						
$7s_{1/2}$	$8p_{1/2}$	28 380.8	1.529[5]	1.847[−2]	1.98	$4d_{3/2}$	$7p_{1/2}$	11 793.3	7.357[5]	7.670[−3]	1.36
$7s_{1/2}$	$8p_{3/2}$	28 229.8	1.790[5]	4.276[−2]	1.78	$4d_{3/2}$	$7p_{3/2}$	11 744.7	7.458[4]	1.542[−3]	1.70
						$4d_{5/2}$	$7p_{3/2}$	11 744.1	6.717[5]	9.259[−3]	1.64
$5p_{1/2}$	$6s_{1/2}$	13 238.8	7.502[6]	1.971[−1]	0.46	$4d_{3/2}$	$8p_{1/2}$	9542.6	3.588[5]	2.449[−3]	0.80
$5p_{3/2}$	$6s_{1/2}$	13 668.7	1.451[7]	2.032[−1]	0.42	$4d_{3/2}$	$8p_{3/2}$	9525.5	3.637[4]	4.947[−4]	1.14
$5p_{1/2}$	$7s_{1/2}$	7282.0	2.381[6]	1.893[−2]	1.14	$4d_{5/2}$	$8p_{3/2}$	9525.1	3.275[5]	2.970[−3]	1.08
$5p_{3/2}$	$7s_{1/2}$	7410.2	4.536[6]	1.867[−2]	1.18	$5d_{3/2}$	$8p_{1/2}$	24 187.3	4.342[5]	1.904[−2]	0.46
$5p_{1/2}$	$8s_{1/2}$	6072.4	1.141[6]	6.308[−3]	1.28	$5d_{3/2}$	$8p_{3/2}$	24 077.5	4.359[4]	3.789[−3]	0.74
$5p_{3/2}$	$8s_{1/2}$	6161.3	2.169[6]	6.173[−3]	1.32	$5d_{5/2}$	$8p_{3/2}$	24 094.7	3.924[5]	2.277[−2]	0.66
$6p_{1/2}$	$7s_{1/2}$	38 515.5	1.509[6]	3.356[−1]	0.36						
$6p_{3/2}$	$7s_{1/2}$	39 700.7	2.905[6]	3.432[−1]	0.30	$4d_{3/2}$	$5f_{5/2}$	10 078.5	7.023[6]	1.604[−1]	1.68
$6p_{1/2}$	$8s_{1/2}$	18 755.6	5.261[5]	2.774[−2]	1.16	$4d_{5/2}$	$5f_{5/2}$	10 078.0	5.023[5]	7.648[−3]	1.64
$6p_{3/2}$	$8s_{1/2}$	19 032.3	9.914[5]	2.692[−2]	1.20	$4d_{5/2}$	$5f_{7/2}$	10 078.0	7.534[6]	1.530[−1]	1.64
						$4d_{3/2}$	$6f_{5/2}$	8871.3	3.856[6]	6.824[−2]	1.22
$5p_{1/2}$	$4d_{3/2}$	14 756.4	1.018[7]	6.648[−1]	1.06	$4d_{5/2}$	$6f_{5/2}$	8870.9	2.757[5]	3.253[−3]	1.16
$5p_{3/2}$	$4d_{3/2}$	15 292.6	1.864[6]	6.535[−2]	1.10	$4d_{5/2}$	$6f_{7/2}$	8870.9	4.136[6]	6.506[−2]	1.16
$5p_{3/2}$	$4d_{5/2}$	15 293.7	1.119[7]	5.888[−1]	1.06	$4d_{3/2}$	$8f_{5/2}$	7927.7	1.529[6]	2.161[−2]	1.68
$5p_{1/2}$	$7d_{3/2}$	5649.3	1.788[6]	1.711[−2]	1.94	$4d_{5/2}$	$8f_{5/2}$	7927.4	1.094[5]	1.031[−3]	1.60
$5p_{3/2}$	$7d_{3/2}$	5726.2	3.784[5]	1.860[−3]	1.82	$4d_{5/2}$	$8f_{7/2}$	7927.4	1.641[6]	2.062[−2]	1.58
$5p_{3/2}$	$7d_{5/2}$	5725.7	2.248[6]	1.657[−2]	1.74	$5d_{3/2}$	$4f_{5/2}$	91 610.2	2.824[5]	5.330[−1]	0.44
$5p_{1/2}$	$8d_{3/2}$	5364.1	1.231[6]	1.062[−2]	1.44	$5d_{5/2}$	$4f_{5/2}$	91 859.4	2.002[4]	2.533[−2]	0.42

the results was studied for the case with the largest correlation correction, the $5d$–$5p$ transition. Even in this extreme case, the difference (1%) was well below quoted uncertainty (3%). Extensive study of the optimal iteration and scaling procedures for the nd states was also carried out in [84]. The results from the second run are given for nd and nf properties listed in the paper. We note that SDpT and SDpTsc data were always fully iterated, thus including the differences in the iteration and scaling procedures into the uncertainty.

The last column of Table II gives relative uncertainties in the final values $Z^{\rm final}$ in %. Our final results and their uncertainties are used to calculate the recommended values of the transition rates, oscillator strengths, lifetimes, and polarizabilities as well as evaluate the uncertainties of these results.

B. Transition rates and oscillator strengths

We combine recommended NIST energies [63] and our final values of the matrix elements listed in Table II to calculate transition rates A and oscillator strengths f. The transition rates are calculated using

$$A_{ab} = \frac{2.026\,13 \times 10^{18}}{\lambda^3} \frac{S}{2j_a+1} {\rm s}^{-1}, \qquad (6)$$

where the wavelength λ is in Å and the line strength $S = d^2$ is in atomic units.

Transition rates A (s^{-1}) and oscillator strengths f for the ns–$n'p$, np–$n's$, np–$n'd$, nd–$n'p$, and nd–$n'f$ transitions in Rb are summarized in Table III. Vacuum wavelengths obtained from NIST energies are also listed for reference. The relative uncertainties in percent are listed in the column labeled "Unc." The relative uncertainties of the transition rates and oscillator strengths are twice of the corresponding matrix element uncertainties since these properties are proportional to the squares of the matrix elements.

C. Lifetimes

We calculated lifetimes of the $6s$–$10s$, $5p_j$–$9p_j$, $4d_j$–$8d_j$, $4f_j$, and $5f_j$ states in Rb using out final values of the dipole matrix elements and NIST energies [63]. The uncertainties in the lifetime values are obtained from the uncertainties in the matrix elements, a large fraction of which is listed in Table II. The comparison of our results with the latest experimental [8,11,16,19,21,22,27–29] and theoretical [21,55] values is given in Table IV. The present lifetimes are in good agreement with experiential results when theoretical and experimental uncertainties are taken into account. The accuracy of the $6s$ lifetime measurement was substantially improved in a recent paper [8] in comparison with older measurements [19] (45.57 ± 0.17 ns [8] instead of 46 ± 5 ns [19]). Our theoretical results for the $6s$ and $5p_j$ lifetimes are in excellent agreement

TABLE IV. Comparison of the Rb lifetimes (in ns) with other theory and experiment. Uncertainties are given in parentheses. References are given in square brackets.

Level	Present	Theory	Expt.
$6s_{1/2}$	45.4(1)	45.4 [55]	45.57(17) [8]
$7s_{1/2}$	88.3(5)	88.3 [55]	88.07(40) [29]
$8s_{1/2}$	161.9(9)	161.8 [55]	161(3) [27]
$9s_{1/2}$	271.7(8)	266.36 [21]	253(14) [19]
$10s_{1/2}$	426(1)	417.84 [21]	430(20) [21]
$5p_{1/2}$	27.4(4)	27.04 [21]	27.75(8) [28]
$5p_{3/2}$	26.0(4)	25.69 [21]	26.25(8) [28]
$6p_{1/2}$	122.5(2.2)	123 [55]	125(4) [19]
$6p_{3/2}$	112.4(1.7)	113 [55]	112(3) [19]
$7p_{1/2}$	277.8(4.3)	280 [55]	272(15) [19]
$7p_{3/2}$	255.2(3.4)	258 [55]	246(10) [19]
$8p_{1/2}$	501.0(4.1)	508 [55]	
$8p_{3/2}$	464.2(3.2)	471 [55]	400(80) [21]
$9p_{1/2}$	809.3(2.9)	798.84 [21]	
$9p_{3/2}$	753.8(2.8)	749.21 [21]	665(40) [19]
$4d_{3/2}$	83.0(0.8)	83.5 [55]	86(6) [21]
$4d_{5/2}$	89.4(0.9)	90 [55]	94(6) [21]
$5d_{3/2}$	240.3(7.3)	243 [55]	246.3(1.6) [11]
$5d_{5/2}$	231.6(8.2)	235 [55]	238.5(2.3) [11]
$6d_{3/2}$	258.0(5.3)	263 [55]	256(4) [27]
$6d_{5/2}$	247.4(5.5)	252 [55]	249(5) [27]
$7d_{3/2}$	339.5(4.3)	331.08 [21]	345(9) [22]
$7d_{5/2}$	327.0(4.4)	319.57 [21]	325(22) [19]
$8d_{3/2}$	468.8(4.2)	455.48 [21]	515(30) [16]
$8d_{5/2}$	452.7(4.3)	440.90 [21]	421(25) [19]
$4f_{5/2}$	60.7(2.2)	59.44 [21]	
$4f_{7/2}$	60.8(2.1)	59.44 [21]	
$5f_{5/2}$	109.3(1.8)	106.12 [21]	
$5f_{7/2}$	109.4(1.7)	106.09 [21]	

with recent precision measurements reported in [8] and [28], respectively.

The lifetimes of the $5d$ states are particularly difficult to calculate accurately owing to very large correlation contributions to the $5p$–$5d$ matrix elements. For example, DHF value for the $5d_{5/2}$–$5p_{3/2}$ matrix element is 0.439 a.u. while our final value is 1.982 a.u. There are only two decay channels ($5d_{5/2}$–$5p_{3/2}$ and $5d_{5/2}$–$6p_{3/2}$) in the case of the $5d_{5/2}$ level, and the $5d_{5/2}$–$5p_{3/2}$ channel contributes 67%. As a result, the uncertainty of the $5d$ lifetime is dominated by the uncertainty in the $5d_{5/2}$–$5p_{3/2}$ matrix element, which is 2.6%. As we noted above, the uncertainty in the respective transition rate is twice that of the matrix element. There are four decay channels ($5d_{3/2}$–$5p_j$ and $5d_{3/2}$–$6p_j$) in the case of the $5d_{3/2}$ level, and combined $5d_{3/2}$–$5p_j$ contribution is 63%. Nevertheless, our values are in agreement with recent measurements [11] taking into account the uncertainties of our values. Lifetime measurements of the $5d_{3/2}$ and $5d_{5/2}$ states of rubidium were performed using the time-correlated single-photon-counting method [11]. The 761.9-nm fluorescence from the decay of the $5d_{3/2}$ state to the $5p_{1/2}$ state was recorded, and resulting value of the lifetime of the $5d_{3/2}$ state was reported to be $\tau = 246.3 \pm 1.6$ ns. Authors recorded the 420.2-nm fluorescence from the cascade decay of the $5d_{5/2}$ state to the $5s_{1/2}$ state through the $6p_{3/2}$ state and extracted the lifetime of the $5d_{5/2}$ state to be $\tau = 238.5 \pm 2.3$ ns. These measurements represent more than an order-of-magnitude improvement in comparison with older experiments (the lifetime of the $5d_{5/2}$ level reported by Marek and Munster in Ref. [19] was equal to 230 ± 23 ns, while the lifetime of the $5d_{3/2}$ level reported by Tai *et al.* in Ref. [14] was equal to 205 ± 40 ns). Small differences between our present results and all-order calculations from Ref. [55] are due to differences in the iteration procedure discussed in the previous section and are generally within the quoted uncertainties.

We observe some disagreement between our data and older, less accurate experimental results. For example, our theoretical lifetime for the $8d_{3/2}$ level (468.8 ± 4.2 ns) differs by 10% from the experimental lifetime (515 ± 30 ns) in Ref. [16]. It should be noted that another experimental lifetime obtained 15 years later [22] gave an even larger value (586 ± 15 ns). Our theoretical value for the the $8d_{3/2}$ lifetime is in good agreement with theoretical value (455.48 ns) given by Theodosiou [21]. The difference in evaluations of the $5p_{3/2}$ and $8d_{3/2}$ lifetimes is in increasing of the number of transitions in the case of the $8d_{3/2}$ level. We need to consider the 10 $np_j - 8d_{3/2}$ transitions with $n = 5$–9 and $j = 1/2$ and $3/2$ and the 3 $nf_{5/2}$–$8d_{3/2}$ transitions with $n = 4$–6. The major contribution (70%) in the sum of transition rates used in the evaluation of the $8d_{3/2}$ lifetime comes from the sum of the $5p_{1/2}$–$8d_{3/2}$ and $5p_{3/2}$–$8d_{3/2}$ transitions rates. The sum of the $6p_{1/2}$–$8d_{3/2}$ and $6p_{3/2}$–$8d_{3/2}$ transitions rates brings an additional 12%. The $nf_{5/2}$–$8d_{3/2}$ transitions with $n = 4$–6 contribute another 12%. The last 6% contribution comes from the np_j–$8d_{3/2}$ transitions with $n = 7$–9 and $j = 1/2$ and $3/2$. New, more accurate, measurements of such lifetimes would provide excellent benchmark tests of theoretical calculations.

IV. STATIC MULTIPOLE POLARIZABILITIES OF THE 5*s* GROUND STATE

The static multipole polarizability α^{Ek} of Rb in its $5s$ ground state can be separated into two terms: a dominant first term from intermediate valence-excited states and a smaller second term from intermediate core-excited states. The later term is smaller than the former one by several orders of magnitude and is evaluated here in the RPA [85]. The dominant valence contribution is calculated using the sum-over-state approach,

$$\alpha_v^{Ek} = \frac{1}{2k+1} \sum_n \frac{\left|\langle nl_j \| r^k C_{kq} \| 5s \rangle\right|^2}{E_{nlj} - E_{5s}}, \tag{7}$$

where $C_{kq}(\hat{r})$ is a normalized spherical harmonic and where nl_j is np_j, nd_j, and nf_j for $k = 1$, 2, and 3, respectively [86]. The reduced matrix elements in the dominant contributions to the above sum are evaluated using final values of the dipole matrix elements and NIST energies [63]. The uncertainties in the polarizability contributions are obtained from the uncertainties in the matrix elements. The final values for the quadrupole and octupole matrix elements and their uncertainties are determined using the procedure that was described above for the dipole matrix elements.

Contributions to dipole, quadrupole, and octupole polarizabilities of the $5s$ ground state are presented in Table V.

TABLE V. Contributions to multipole polarizabilities of the 5*s* state of rubidium in a_0^3. Uncertainties are given in parentheses. The final results are compared with other theory [39,40] and experiment [34,35].

Contr.	α^{E1}
$5p_{1/2}$	105(2)
$5p_{3/2}$	206(3)
(6–26)p_j	2(0)
Tail	−0.3
Core	9.1
Total	322(4)
$\alpha^{E1}_{\rm th}$ [39]	316.4
$\alpha^{E1}_{\rm expt}$ [35]	319(6)
$\alpha^{E1}_{\rm expt}$ [34]	329(23)
Contr.	α^{E2}
$4d_{3/2}$	2461(21)
(5–12)$d_{3/2}$	26(0)
(13–26)$d_{3/2}$	120(0)
$4d_{5/2}$	3696(31)
(5–12)$d_{5/2}$	37
(13–26)$d_{5/2}$	148
Tail	1.8
Core	35.4
Total	6525(37)
$\alpha^{E2}_{\rm th}$ [40]	6520 ± 80
Contr.	α^{E3}
$4f_{5/2}$	50 012(920)
$5f_{5/2}$	16 015(173)
$6f_{5/2}$	7002(80)
$7f_{5/2}$	3708(43)
$8f_{5/2}$	2218(26)
(9–12)$f_{5/2}$	5006
(13–18)$f_{5/2}$	8361
(19–26)$f_{5/2}$	9301
$4f_{7/2}$	66 685(1276)
$5f_{7/2}$	21 354(231)
$6f_{7/2}$	9336(106)
$7f_{7/2}$	4944 (57)
$8f_{7/2}$	2957 (34)
(9–12)$f_{7/2}$	6674
(13–18)$f_{7/2}$	12 352
(19–26)$f_{7/2}$	11 194
Tail	22
Core	306
Total	237 400(1600)
$\alpha^{E2}_{\rm th}$ [40]	237 000

The first two terms in the sum-over-states for α^{E1}, α^{E2}, and α^{E3} contribute 99.4%, 94.18%, and 48.2%, respectively, of the totals. The remaining 6% of α^{E2} contribution from the (5–26)nd_j states is divided into two parts, resulting from (5–12)nd_j and (13–26)nd_j states. Finally, the 48% of α^{E3} contribution from the (5–26)nf_j states are split in Table V into seven contributions coming from the $5f_j$, $6f_j$, $7f_j$, $8f_j$, (9–12)n_j, (13–18)nd_j, and (19–26)nd_j states to show the relative importance of these terms. We use recommended energies from [63] and our final matrix elements to evaluate terms in the sum with $n \leqslant 13$, and we use theoretical SD energies and wave functions to evaluate terms with $13 \leqslant n \leqslant 26$. The remaining contributions to α^{Ek} from orbitals with $27 \leqslant n \leqslant 70$ are evaluated in the DF approximation since the contributions from these terms are smaller than 0.01% in all cases. These terms are grouped together as "Tail".

Final results for the multipole polarizabilities of the Rb ground state are compared in Table V with high-precision calculations from Refs. [39,40] and experimental measurements presented in Refs. [34,35]. Our results agree with values given by Derevianko *et al.* [39] for the dipole polarizability taking into account the uncertainty given in [39]. Our recommended values for the quadrupole and octupole polarizabilities are in agreement with values of Ref. [40].

V. SCALAR AND TENSOR EXCITED-STATE POLARIZABILITIES

The valence scalar $\alpha_0(v)$ and tensor $\alpha_2(v)$ polarizabilities of an excited state v of Rb are given by

$$\alpha_0(v) = \frac{2}{3(2j_v+1)} \sum_{nlj} \frac{|\langle v||rC_1||nlj\rangle|^2}{E_{nlj} - E_v}, \tag{8}$$

$$\alpha_2(v) = (-1)^{j_v} \sqrt{\frac{40 j_v (2j_v-1)}{3(j_v+1)(2j_v+1)(2j_v+3)}} \times \sum_{nlj} (-1)^j \begin{Bmatrix} j_v & 1 & j \\ 1 & j_v & 2 \end{Bmatrix} \frac{|\langle v||rC_1||nlj\rangle|^2}{E_{nlj} - E_v}. \tag{9}$$

The excited state polarizability calculations are carried out in the same way as the calculations of the multipole polarizabilities discussed in the previous section. We list the contributions to the $6s$, $7s$, $8s$, $9s$, $10s$, $5p_j$, $6p_j$, $7p_j$, $4d_j$, $5d_j$, and $6d_j$ scalar polarizabilities of Rb in Table VI. The dominant contributions are listed separately. The remaining contributions are grouped together. For example, "$nd_{3/2}$" contribution includes all of the $nd_{3/2}$ terms excluding only the terms that were already listed separately. We evaluate contribution from ionic core $\alpha_{\rm core}$ in the RPA and find $\alpha_{\rm core} = 9.076 a_0^3$.

Contributions from the np states with $n \leqslant 26$ to the ns polarizabilities are so small in comparison with the main contributions that we group them together with the $\alpha_{\rm core}$ contribution in the line labeled "Other". Contributions from excited ns and nd states with $n > 26$ to the np polarizability are very small $\alpha_{n>26}(5p_{1/2}) = 0.061 a_0^3$, $\alpha_{n>26}(5p_{3/2}) = 0.048 a_0^3$ and are calculated in the RPA approximation. Contributions from the excited np and nf states with $n \leqslant 26$ to the nd polarizabilities are only 10^{-4} a.u. A counterterm $\alpha_{\rm vc}(n_j)$ compensating for excitation from the core to the valence shell which violate the Pauli principle is also evaluated in the RPA and found to be negligible. The largest contribution of the $\alpha_{\rm vc}$ term is for the $4d$ states [$\alpha_{\rm vc}(4d_{3/2}) = -0.085\ a_0^3$ and $\alpha_{\rm vc}(4d_{5/2}) = -0.097\ a_0^3$].

Final results of the scalar dipole polarizabilities are compared in Table VI with semi-empirical values of van Wijngaarden [38] where a Coulomb approximation was used.

TABLE VI. Contributions to the $6s$–$10s$, $5p_j$–$7p_j$, and $4d_j$–$6d_j$ scalar polarizabilities of Rb in a_0^3. $n_1 f_{7/2} = (7\text{–}12) f_{7/2}$, $n_2 f_{7/2}$ includes $nf_{7/2}$ states with $n > 13$. Uncertainties are given in parentheses. The final results are compared with other theory [7,38].

Contr.	α_0	Contr.	α_0	Contr.	α_0	Contr.	α_0	Contr.	α_0	Contr.	α_0
	$6s_{1/2}$		$7s_{1/2}$		$8s_{1/2}$		$9s_{1/2}$		$10s_{1/2}$		
$5p_{1/2}$	−166(1)	$6p_{1/2}$	−2398(9)	$7p_{1/2}$	−15424(0)	$8p_{1/2}$	−66 575(280)	$9p_{1/2}$	−220 569(926)		
$5p_{3/2}$	−365(2)	$6p_{3/2}$	−5212(16)	$7p_{3/2}$	−33 540(107)	$8p_{3/2}$	−143 462(545)	$9p_{3/2}$	−474 280(1802)		
$6p_{1/2}$	1930(10)	$7p_{1/2}$	13 695(66)	$8p_{1/2}$	62170(298)	$9p_{1/2}$	214 534(987)	$10p_{1/2}$	612 959(2697)		
$6p_{3/2}$	3722(19)	$7p_{3/2}$	26 263(126)	$8p_{3/2}$	11 8801(570)	$9p_{3/2}$	408 987(1881)	$10p_{3/2}$	1 166 324(5365)		
Other	49(1)	Other	285(5)	Other	1174(22)	Other	3691(72)	Other	976 (184)		
Total	5169(21)	Total	32 630(140)	Total	133 200(650)	Total	417 200(2200)	Total	1 094 000(6000)		
[38]	5110		32 400		132 000		416 000		1 090 000		
[7]							417 040(360)		1 095 310(640)		
	$5p_{1/2}$		$6p_{1/2}$		$7p_{1/2}$		$4d_{3/2}$		$5d_{3/2}$		$6d_{3/2}$
$5s_{1/2}$	−105(2)	$6s_{1/2}$	−1930(10)	$7s_{1/2}$	−13 695(66)	$5p_{1/2}$	−347(4)	$6p_{1/2}$	−6100(59)	$7p_{1/2}$	−42 366(119)
$6s_{1/2}$	166(1)	$7s_{1/2}$	2398(9)	$8s_{1/2}$	15424	$6p_{1/2}$	226(14)	$7p_{1/2}$	1910(91)	$8p_{1/2}$	9982(323)
$7s_{1/2}$	5	$8s_{1/2}$	47(1)	$9s_{1/2}$	247(3)	$5p_{3/2}$	−74(1)	$6p_{3/2}$	−1291(9)	$7p_{3/2}$	−8983(25)
$ns_{1/2}$	4	$ns_{1/2}$	25(0)	$ns_{1/2}$	90(1)	$6p_{3/2}$	42(3)	$7p_{3/2}$	356(18)	$8p_{3/2}$	1856(62)
$4d_{3/2}$	697(7)	$4d_{3/2}$	−452(29)	$5d_{3/2}$	−3820(183)	np_j	10(0)	np_j	22(1)	np_j	468(6)
$5d_{3/2}$	10(1)	$5d_{3/2}$	12 199(117)	$6d_{3/2}$	84 733(237)	$4f_{5/2}$	534(21)	$4f_{5/2}$	21 546(95)	$5f_{5/2}$	132 300(529)
$6d_{3/2}$	5	$6d_{3/2}$	37(3)	$7d_{3/2}$	94(9)	$5f_{5/2}$	78(1)	$5f_{5/2}$	898(54)	$6f_{5/2}$	1410(9)
$nd_{3/2}$	22(0)	$nd_{3/2}$	86(1)	$nd_{3/2}$	191(2)	$nf_{5/2}$	97(1)	$nf_{5/2}$	464(15)	$nf_{5/2}$	−765(38)
Core	9	Core	9	Core	9	Core	9	Core	9	Core	9
Total	814(8)	Total	12 420(120)	Total	83 270(300)	Total	574(25)	Total	17 880(160)	Total	93 900(600)
[38]	805		12 600		83 600		571		18 700		96 000
	$5p_{3/2}$		$6p_{3/2}$		$7p_{3/2}$		$4d_{5/2}$		$5d_{5/2}$		$6d_{5/2}$
$5s_{1/2}$	−103(2)	$6s_{1/2}$	−1861(9)	$7s_{1/2}$	−13 131(63)	$5p_{3/2}$	−442(5)	$6p_{3/2}$	−7736(50)	$7p_{3/2}$	−53 742(140)
$6s_{1/2}$	183(1)	$7s_{1/2}$	2606(8)	$8s_{1/2}$	16 770(54)	$6p_{3/2}$	254(16)	$7p_{3/2}$	2149(102)	$8p_{3/2}$	11 230(353)
$7s_{1/2}$	5(0)	$8s_{1/2}$	47(1)	$9s_{1/2}$	244(3)	$np_{3/2}$	10(0)	$np_{3/2}$	88(0)	$np_{3/2}$	460(6)
$ns_{1/2}$	4(0)	$ns_{1/2}$	24(0)	$ns_{1/2}$	96(1)4	$4f_{5/2}$	25(1)	$4f_{5/2}$	1029(4)	$4f_{5/2}$	−80(1)
$4d_{3/2}$	74(1)	$4d_{3/2}$	−42(3)	$5d_{3/2}$	−356(18)	$5f_{5/2}$	4(0)	$5f_{5/2}$	43(2)	$5f_{5/2}$	6330(24)
$5d_{3/2}$	1(0)	$5d_{3/2}$	1291(9)	$6d_{3/2}$	8983(25)	$6f_{5/2}$	1(0)	$6f_{5/2}$	9(0)	$6f_{5/2}$	69(4)
$6d_{3/2}$	0(0)	$6d_{3/2}$	5(0)	$7d_{3/2}$	14(1)	$nf_{5/2}$	3(0)	$nf_{5/2}$	13(0)	$nf_{5/2}$	44(1)
$nd_{3/2}$	2(0)	$nd_{3/2}$	10(0)	$nd_{3/2}$	22(0)	$4f_{7/2}$	509(19)	$4f_{7/2}$	20 588(86)	$4f_{7/2}$	−1594(20)
$4d_{5/2}$	663(7)	$4d_{5/2}$	−381(24)	$5d_{5/2}$	−3224(153)	$5f_{7/2}$	75(1)	$5f_{7/2}$	862(49)	$5f_{7/2}$	126 595(481)
$5d_{5/2}$	11(1)	$5d_{5/2}$	11 604(74)	$6d_{5/2}$	80 613(210)	$6f_{7/2}$	25(0)	$6f_{7/2}$	187(6)	$6f_{7/2}$	1372(81)
$6d_{5/2}$	5(0)	$6d_{5/2}$	45(3)	$7d_{5/2}$	125(10)	$n_1 f_{7/2}$	31(0)	$n_1 f_{7/2}$	158(8)	$n_1 f_{7/2}$	701(14)
$nd_{5/2}$	19(0)	$nd_{5/2}$	83(1)	$nd_{5/2}$	195(2)	$n_2 f_{7/2}$	37(0)	$n_2 f_{7/2}$	100(0)	$n_2 f_{7/2}$	184(0)
Core	9	Core	9	Core	9	Core	9	Core	9	Core	9
Total	875(7)	Total	13 440(70)	Total	90 350(270)	Total	541(26)	Total	17 500(150)	Total	91 580(620)
[38]	868		13 600		90 600		535		18 300		93 600

These results [38] are in good agreement with our calculations. The differences are about 0.3% for the polarizabilities of the ns and np states. Larger differences are observed for the nd states (1.5% for the $4d_j$ states and 5% for the $5d_j$ states). It is expected owing to generally larger contributions of the correlation corrections to the nd states and our more complete treatment of the correlation corrections.

Our final results are in excellent agreement with recent precision measurements reported in Refs. [7] [0.26% difference for the $\alpha(9s)$ and 0.35% difference for the $\alpha(10s)$].

A breakdown of contributions to the tensor dipole polarizability α_2 for the excited $np_{3/2}$ ($n = 5$, 6, and 7) and nd_j ($n = 4$, 5, and 6) states is presented in Table VII. Evaluation of the tensor polarizability follows the same pattern as the scalar polarizability [compare Eqs. (8) and (9)]. The difference in evaluations of the α_0 and α_2 values is in the angular part only. States with $n > 13$ in our basis have positive energies and provide a discrete representation of the continuum. We find that the continuous part of the spectra is responsible for 2% of $\alpha_2(5p_{3/2})$. We have evaluated the continuum contributions and near-continuum contributions in the range $11 < n \leqslant 26$ using SD wave functions for dipole matrix elements. For $n \leqslant 11$, we use SD matrix elements and NIST energies [63] in the sums. Contributions from states with $n > 26$ is negligible (about 10^{-4} %). Our final results for α_2 are given in Table VII. We observe very strong cancelations of dominant terms in many of the tensor polarizabilities, resulting in larger uncertainties in our values. Final results for the tensor polarizabilities α_2 are compared in Table VII with semiempirical values of van Wijngaarden [38] where a Coulomb approximation was used. The agreement between our results and semiempirical values from Ref. [38] is at

TABLE VII. Contributions to the $np_{3/2}$ and nd_j tensor polarizabilities of Rb in units of a_0^3. Uncertainties are given in parentheses. The final results are compared with other theory [38].

Contr.	α_2	Contr.	α_2	Contr.	α_2
	$5p_{3/2}$		$6p_{3/2}$		$7p_{3/2}$
$5s_{1/2}$	103(2)	$6s_{1/2}$	1861(9)	$7s_{1/2}$	13 131(63)
$6s_{1/2}$	−183(1)	$7s_{1/2}$	−2606(8)	$8s_{1/2}$	−16 770(54)
$7s_{1/2}$	−5(0)	$8s_{1/2}$	−47(0)	$9s_{1/2}$	−244(3)
$ns_{1/2}$	4(0)	$ns_{1/2}$	−24(0)	$ns_{1/2}$	−84(0)
$4d_{3/2}$	59(1)	$4d_{3/2}$	−33(2)	$5d_{3/2}$	−285(14)
$5d_{3/2}$	1(0)	$5d_{3/2}$	1032(7)	$6d_{3/2}$	7186(20)
$6d_{3/2}$	0(0)	$6d_{3/2}$	4(0)	$7d_{3/2}$	12(1)
$nd_{3/2}$	2(0)	$nd_{3/2}$	8(0)	$nd_{3/2}$	20(0)
$4d_{5/2}$	−133(1)	$4d_{5/2}$	76(4)	$5d_{5/2}$	645(31)
$5d_{5/2}$	−2(0)	$5d_{5/2}$	−2321(15)	$6d_{5/2}$	−16 123(42)
$6d_{5/2}$	−1(0)	$6d_{5/2}$	−9(1)	$7d_{5/2}$	−25(2)
$nd_{5/2}$	−4(0)	$nd_{5/2}$	−17(0)	$nd_{5/2}$	−39(0)
Total	−167(2)		−2075(21)		−12 577(101)
Ref. [38]	−143		−2040		−12 500
	$4d_{3/2}$		$5d_{3/2}$		$6d_{3/2}$
$5p_{1/2}$	349(4)	$6p_{1/2}$	6100(59)	$7p_{1/2}$	42 366(118)
$6p_{1/2}$	−226(2)	$7p_{1/2}$	−1910(30)	$8p_{1/2}$	−9982(51)
$7p_{1/2}$	−5(0)	$8p_{1/2}$	−54(0)	$9p_{1/2}$	−289(2)
$np_{1/2}$	−3(0)	$np_{1/2}$	−21(0)	$np_{1/2}$	−103(0)
$5p_{3/2}$	−59(1)	$6p_{3/2}$	−1032(7)	$7p_{3/2}$	−7186(20)
$6p_{3/2}$	34(0)	$7p_{3/2}$	285(5)	$8p_{3/2}$	1485(24)
$7p_{3/2}$	1(0)	$8p_{3/2}$	8(0)	$9p_{3/2}$	46(0)
$np_{3/2}$	0(0)	$np_{3/2}$	3(0)	$np_{3/2}$	15(0)
$4f_{5/2}$	−107(4)	$4f_{5/2}$	−4309(19)	$4f_{5/2}$	337(4)
$5f_{5/2}$	−16(0)	$5f_{5/2}$	−180(11)	$5f_{5/2}$	−26 460(106)
$6f_{5/2}$	−5(0)	$6f_{5/2}$	−39(1)	$6f_{5/2}$	−284(18)
$nf_{5/2}$	−14(0)	$nf_{5/2}$	−54(0)	$nf_{5/2}$	−184(0)
Total	−51(6)		−1203(70)		−238(223)
Ref. [38]	−49		−1300		−559
	$4d_{5/2}$		$5d_{5/2}$		$6d_{5/2}$
$5p_{3/2}$	442(5)	$6p_{3/2}$	7736(50)	$7p_{3/2}$	53 742(140)
$6p_{3/2}$	−254(3)	$7p_{3/2}$	−2149(36)	$8p_{3/2}$	−11 230(173)
$7p_{3/2}$	−6(0)	$8p_{3/2}$	−64(0)	$9p_{3/2}$	−343(3)
$np_{3/2}$	−4(0)	$np_{3/2}$	−24(0)	$np_{3/2}$	−117(0)
$4f_{5/2}$	29(1)	$4f_{5/2}$	1176(5)	$4f_{5/2}$	−91(1)
$5f_{5/2}$	4(0)	$5f_{5/2}$	49(3)	$5f_{5/2}$	7234(27)
$6f_{5/2}$	1(0)	$6f_{5/2}$	11(0)	$6f_{5/2}$	78(5)
$nf_{5/2}$	4(0)	$nf_{5/2}$	15(0)	$nf_{5/2}$	51(0)
$4f_{7/2}$	−181(6)	$4f_{7/2}$	−7353(31)	$4f_{7/2}$	569(7)
$5f_{7/2}$	−26(0)	$5f_{7/2}$	−308(18)	$5f_{7/2}$	−45 213(172)
$6f_{7/2}$	−8(0)	$6f_{7/2}$	−67(2)	$6f_{7/2}$	−490(29)
$nf_{7/2}$	−24(0)	$nf_{7/2}$	−92(0)	$nf_{7/2}$	−316(0)
Total	−24(9)		−1070(71)		3875(284)
Ref. [38]	−18.3		−1200		3450

the level of 1% for the $6p_{3/2}$ and $4d_{3/2}$ states. For all other states ($5p_{3/2}$, $4d_{5/2}$, $5d_{3/2}$, and $5d_{5/2}$), the differences are about 10%.

VI. HYPERFINE CONSTANTS FOR ^{87}RB

Calculations of hyperfine constants follow the pattern described earlier for calculations of transition matrix elements. In

TABLE VIII. Hyperfine constants A (in MHz) in ^{87}Rb ($I = 3/2$, $\mu = 2.75124$ [87]). The SD and SDpT (single-double all-order method including partial triple excitations) data are compared with experimental results.

Level	$A^{(\mathrm{DF})}$	$A^{(\mathrm{SD})}$	$A^{(\mathrm{SDpT})}$	$A^{(\mathrm{expt})}$
$5s\ ^2S_{1/2}$	2175.98	3563.40	3417.25	3417.341 [45]
$5p\ ^2P_{1/2}$	236.71	425.65	408.53	406.2(8) [45]
$5p\ ^2P_{3/2}$	42.05	86.53	83.14	84.845(55) [45]
$6s\ ^2S_{1/2}$	581.17	824.40	806.06	807.66(8) [10]
$6p\ ^2P_{1/2}$	83.19	136.31	132.34	132.56(3) [45]
$6p\ ^2P_{3/2}$	14.83	27.84	27.03	27.700(17) [45]
$7s\ ^2S_{1/2}$	238.06	324.87	319.20	319.759(28) [9]
$7p\ ^2P_{1/2}$	38.59	61.33	59.78	59.32(3) [45]
$7p\ ^2P_{3/2}$	6.89	12.55	12.23	12.57(1) [45]
$8s\ ^2S_{1/2}$	120.22	161.12	158.66	159.2(15) [45]
$8p\ ^2P_{1/2}$	20.97	32.82	32.05	32.12(11) [45]
$8p\ ^2P_{3/2}$	3.75	6.72	6.57	6.739(15) [45]
$9s\ ^2S_{1/2}$	69.02	91.52	90.23	90.9(8) [45]
$9p\ ^2P_{1/2}$	12.63	19.59		
$9p\ ^2P_{3/2}$	2.26	4.02		4.05(3) [45]
$4d\ ^2D_{3/2}$	10.36	26.58	29.66	25.1(9) [45]
$4d\ ^2D_{5/2}$	4.42	−13.66	−16.52	−16.9(6) [45]
$5d\ ^2D_{3/2}$	6.49	15.24	16.57	14.43(23) [45]
$5d\ ^2D_{5/2}$	2.75	−6.18	−7.07	−7.44(10) [45]
$6d\ ^2D_{3/2}$	3.75	8.18	8.76	7.84(5) [45]
$6d\ ^2D_{5/2}$	1.59	−2.97	−3.30	−3.4(5) [45]
$7d\ ^2D_{3/2}$	2.28	4.74	5.04	4.53(3) [45]
$7d\ ^2D_{5/2}$	0.96	−1.62	−1.78	−2.0(3) [45]
$8d\ ^2D_{3/2}$	1.46	2.96	3.13	2.840(15) [45]
$8d\ ^2D_{5/2}$	0.62	−0.97	−1.06	−1.20(15) [45]
$9d\ ^2D_{3/2}$	0.99	1.97	2.07	1.90(1) [45]
$9d\ ^2D_{5/2}$	0.42	−0.63	−0.69	−0.80(15) [45]

Table VIII, we list hyperfine constants A for ^{87}Rb and compare our values with available experimental data from Refs. [45]. In this table, we present the lowest-order $A^{(\mathrm{DF})}$, all-order $A^{(\mathrm{SD})}$, and $A^{(\mathrm{SDpT})}$ values for the ns, np, and nd levels up to $n = 9$. The magnetic moment and nuclear spin of ^{87}Rb used here are

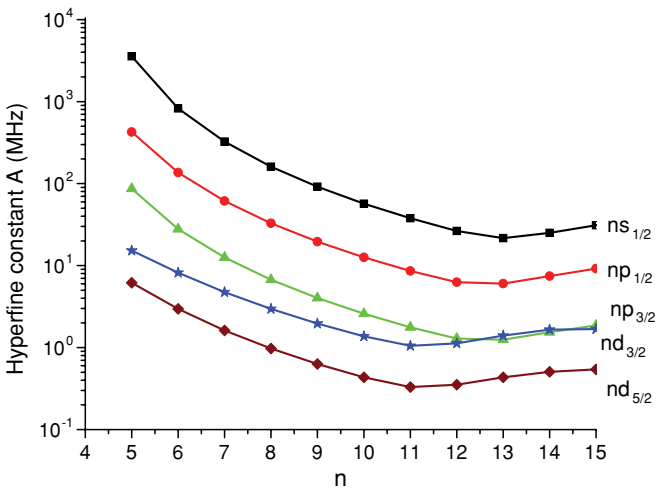

FIG. 1. (Color online) Hyperfine constant $A^{(\mathrm{SD})}(nlj)$ as a function of n.

TABLE IX. Hyperfine constants B (in MHz) in ^{87}Rb ($I = 3/2$, $\mu = 2.75124$ [87]). Nuclear quadrupole moment Q equal to 0.132 in barns (1 b $= 10^{-24}$ cm^2) [88]. The SD and SDpT (single-double all-order method including partial triple excitations) data are compared with experimental results.

Level	$\frac{B^{(\mathrm{DF})}}{Q}$	$\frac{B^{(\mathrm{SD})}}{Q}$	$\frac{B^{(\mathrm{SDpT})}}{Q}$	$B^{(\mathrm{DF})}$	$B^{(\mathrm{SD})}$	$B^{(\mathrm{SDpT})}$	$B^{(\mathrm{expt})}$
$5p\ ^2P_{3/2}$	43.17	93.87	93.87	5.699	12.391	11.967	12.52(9) [45]
$6p\ ^2P_{3/2}$	15.20	29.32	29.32	2.006	3.870	3.772	3.953(24) [45]
$7p\ ^2P_{3/2}$	7.05	13.04	13.04	0.930	1.722	1.684	1.762(16) [45]
$8p\ ^2P_{3/2}$	3.82	6.93	6.93	0.504	0.915	0.896	0.935(22) [45]
$9p\ ^2P_{3/2}$	2.29	4.11	4.11	0.302	0.543		0.55(3) [45]
$4d\ ^2D_{3/2}$	3.49	16.87	16.87	0.461	2.227	2.230	
$4d\ ^2D_{5/2}$	4.90	23.93	23.93	0.647	3.159	3.166	
$5d\ ^2D_{3/2}$	2.17	6.90	6.90	0.287	0.911	0.913	
$5d\ ^2D_{5/2}$	3.03	9.73	9.73	0.400	1.285	1.290	
$6d\ ^2D_{3/2}$	1.24	3.33	3.33	0.164	0.440	0.442	0.53(6) [45]
$6d\ ^2D_{5/2}$	1.72	4.69	4.69	0.228	0.619	0.623	
$7d\ ^2D_{3/2}$	0.74	1.83	1.83	0.097	0.242	0.243	0.26(4) [45]
$7d\ ^2D_{5/2}$	1.02	2.58	2.58	0.135	0.341	0.343	
$8d\ ^2D_{3/2}$	0.46	1.11	1.11	0.061	0.146	0.147	0.17(2) [45]
$8d\ ^2D_{5/2}$	0.64	1.56	1.56	0.084	0.205	0.207	
$9d\ ^2D_{3/2}$	0.30	0.71	0.71	0.039	0.094	0.094	0.11(3) [45]
$9d\ ^2D_{5/2}$	0.41	1.00	1.00	0.055	0.132	0.133	

taken from [87]. The importance of the triple excitations for accurate evaluation of the hyperfine constants was previously discussed in Ref. [71], and we take our SDpT values as final. Our SDpT results are in very good agreement with experimental values for the ns and $np_{1/2}$ states. Our $A^{(\mathrm{SDpT})}$ values for the $7s$ and $6s$ states are in the excellent agreement with recent measurements [9,10]. The difference between theory and experiment is equal to 0.17% for the $7s$ state and 0.07% for the $6s$ state.

The correlation correction for the $nd_{5/2}$ states is of the same order of magnitude as the DF value and has an opposite sign. With such large cancelations, it is difficult to calculate $A(nd_{5/2})$ accurately. However, we find good agreement between our $A^{(\mathrm{SDpT})}$ values and experimental values [45], except for the $5d_{5/2}$ state, where the disagreement is about 4%.

Finally, we would like to demonstrate very smooth dependence of the $A^{(\mathrm{SD})}$ hyperfine constants on the principal quantum number n. In Fig. 1, we present our $A^{(\mathrm{SD})}$ values for the ns, $np_{1/2}$, $np_{3/2}$, $nd_{3/2}$, and $nd_{5/2}$ levels with $n =$ 4–13. It should be noted that the values of $A^{(\mathrm{SD})}(nd_{5/2})$ are shown with an opposite sign since we use a logarithmical scale.

Hyperfine constants B (in MHz) in ^{87}Rb ($I = 3/2$, $\mu = 2.75124$ [87]) are given in Table IX. Nuclear quadrupole moment Q equal to 0.132 in barns (1 b $= 10^{-24}$ cm^2) [88]. The SD and SDpT data are compared with experimental results [45].

VII. CONCLUSION

In summary, we carried out a study of Rb atomic properties for the ns, np_j, nd_j, and nf_j ($n \leqslant 10$) states using a high-precision relativistic all-order approach and evaluated uncertainties of our recommended values. The energy values are in excellent agreement with existing experimental data. Reduced matrix elements, oscillator strengths, transition rates, and lifetimes for the first low-lying levels up to $n = 8$ are calculated. Electric-dipole ($5s$–np_j, $n =$ 5–26), electric-quadrupole ($5s$–nd_j, $n =$ 4–26), and electric-octupole ($5s$–nf_j, $n =$ 4–26) matrix elements are calculated to obtain the ground-state $E1$, $E2$, and $E3$ static polarizabilities. Scalar polarizabilities of the ns, np_j, and nd_j states, and tensor polarizabilities of the $np_{3/2}$ and nd_j excited states of Rb are evaluated. Particular care was taken to accurately treat contributions from highly excited states. We evaluate the uncertainties of our calculations for most of the values listed in this work. Hyperfine A and B values are presented for the first low-lying levels up to $n = 9$. This work provides recommended values for a number of atomic properties via a systematic high-precision study for use in planning and analysis of various experiments as well as theoretical modeling.

ACKNOWLEDGMENTS

The work of M.S.S. was supported in part by National Science Foundation Grant No. PHY-07-58088.

[1] B. Butscher, J. Nipper, J. B. Balewski, L. Kukota, V. Bendkowsky, R. Löw, and T. Pfau, Nat. Phys. **6**, 970 (2010).

[2] X. L. Zhang, L. Isenhower, A. T. Gill, T. G. Walker, and M. Saffman, Phys. Rev. A **82**, 030306 (2010).

[3] Y. O. Dudin, A. G. Radnaev, R. Zhao, J. Z. Blumoff, T. A. B. Kennedy, and A. Kuzmich, Phys. Rev. Lett. **105**, 260502 (2010).

[4] S. Tassy, N. Nemitz, F. Baumer, C. Höhl, A. Batär, and A. Görlitz, J. Phys. B **43**, 205309 (2010).

[5] International Committee for Weights and Measures, *Proceedings of the Sessions of the 95th meeting (October 2006)* [http://www.bipm.org/utils/en/pdf/CIPM2006-EN.pdf].

[6] J. Mitroy, M. S. Safronova, and C. W. Clark, J. Phys. B **43**, 202001 (2010).

[7] J. Walls, J. Clarke, S. Cauchi, G. Karkas, H. Chen, and W. A. van Wijngaarden, Eur. Phys. J. D **14**, 9 (2001).

[8] E. Gomez, F. Baumer, A. D. Lange, G. D. Sprouse, and L. A. Orozco, Phys. Rev. A **72**, 012502 (2005).

[9] H.-C. Chui, M.-S. Ko, Y.-W. Liu, J.-T. Shy, J.-L. Peng, and H. Ahn, Opt. Lett. **30**, 842 (2005).

[10] A. Perez Calván, Y. Zhaoa, L. A. Orozco, E. Gómez, A. D. Lange, F. Baumer, and G. D. Sprouse, Phys. Lett. B **655**, 114 (2007).

[11] D. Sheng, A. Perez Galván, and L. A. Orozco, Phys. Rev. A **78**, 062506 (2008).

[12] J. D. Feichtner, J. H. Gallagher, and M. Mizushima, Phys. Rev. **164**, 44 (1967).

[13] R. W. Schmieder and A. Lurio, Phys. Rev. A **2**, 1216 (1970).

[14] C. Tai, W. Happer, and R. Gupta, Phys. Rev. A **12**, 736 (1975).

[15] F. Gounand, P. R. Fournier, J. Cuvellier, and J. Berlande, Phys. Lett. A **59**, 23 (1976).

[16] H. Lundberg and S. Svanberg, Phys. Lett. A **56**, 31 (1976).

[17] B. R. Bulos, R. Gupta, and W. Happer, J. Opt. Soc. Am. **66**, 426 (1976).

[18] U. Teppner and P. Zimmermann, Astron. Astrophys. **64**, 215 (1978).

[19] J. Marek and P. Münster, J. Phys. B **13**, 1731 (1980).

[20] M. A. Rebolledo and J. J. Sanz, Phys. Rev. A **29**, 1938 (1984).

[21] C. E. Theodosiou, Phys. Rev. A **30**, 2881 (1984).

[22] W. A. van Wijngaarden and J. Sagle, Phys. Rev. A **45**, 1502 (1992).

[23] J. Szonert, B. Bieniak, M. Głódź, and M. Piechota, Z. Phys. D **33**, 177 (1995).

[24] U. Volz and H. Schmoranzer, Phys. Scr. T **65**, 48 (1996).

[25] S. A. Ter-Avetisyan, V. O. Papanyan, and A. G. Maloyan, Opt. Spectrosc. **81**, 515 (1996).

[26] J. E. Simsarian, L. A. Orozco, G. D. Sprouse, and W. Z. Zhao, Phys. Rev. A **57**, 2448 (1998).

[27] A. Ekers, M. Glódź, J. Szonert, B. Bieniak, K. Fronc, and T. Radelitski, Eur. Phys. J. D **8**, 49 (2000).

[28] R. F. Gutterres, C. Amiot, A. Fioretti, C. Gabbanini, M. Mazzoni, and O. Dulieu, Phys. Rev. A **66**, 024502 (2002).

[29] E. Gomez, S. Aubin, L. A. Orozco, and G. D. Sprouse, J. Opt. Soc. Am. B **21**, 2058 (2004).

[30] E. A. Rotberg, B. Barrett, S. Beattie, S. Chudasama, M. Weel, I. Chan, and A. Kumarakrishnan, J. Opt. Soc. Am. B **24**, 671 (2007).

[31] V. A. Zilitis, Opt. Spectrosc. **103**, 895 (2007).

[32] V. A. Zilitis, Opt. Spektrosk. **103**, 931 (2007).

[33] S. Svanberg, Phys. Scr. **5**, 132 (1972).

[34] W. D. Hall and J. C. Zorn, Phys. Rev. A **10**, 1141 (1974).

[35] R. W. Molof, H. L. Schwartz, T. M. Miller, and B. Bederson, Phys. Rev. A **10**, 1131 (1974).

[36] W. Hogervorst and S. Svanberg, Phys. Scr. **12**, 67 (1975).

[37] K. Fredriksson and S. Svanberg, Z. Phys. A **281**, 189 (1977).

[38] W. A. Van Wijngaarden, J. Quant. Spectrosc. Radiat. Transfer **57**, 275 (1997).

[39] A. Derevianko, W. R. Johnson, M. S. Safronova, and J. F. Babb, Phys. Rev. Lett. **82**, 3589 (1999).

[40] S. G. Porsev and A. Derevianko, J. Chem. Phys. **119**, 844 (2003).

[41] A. Khadjavi, A. Lurio, and W. Happer, Phys. Rev. **167**, 128 (1968).

[42] R. Gupta, S. Chang, C. Tai, and W. Happer, Phys. Rev. Lett. **29**, 695 (1972).

[43] R. Gupta, W. Happer, L. K. Lam, and S. Svanberg, Phys. Rev. A **8**, 2792 (1973).

[44] S. Svanberg and P. Tsekeris, Phys. Rev. A **11**, 1125 (1975).

[45] E. Arimondo, M. Inguscio, and P. Violino, Rev. Mod. Phys. **49**, 31 (1977).

[46] W. A. Van Wijngaarden, K. D. Bonin, and W. Happer, Phys. Rev. A **33**, 77 (1986).

[47] W. A. Van Wijngaarden and J. Sagle, J. Phys. B **24**, 897 (1991).

[48] W. A. van Wijngaarden, J. Li, and J. Koh, Phys. Rev. A **48**, 829 (1993).

[49] M. J. Snadden, A. Bell, E. Riis, and A. Ferguson, Opt. Commun. **125**, 70 (1996).

[50] E. J. Angstmann, V. A. Dzuba, and V. V. Flambaum, Phys. Rev. A **74**, 023405 (2006).

[51] W. R. Johnson, Z. W. Liu, and J. Sapirstein, At. Data Nucl. Data Tables **64**, 279 (1996).

[52] E. Eliav, U. Kaldor, and Y. Ishikawa, Phys. Rev. A **50**, 1121 (1994).

[53] E. Eliav, M. J. Vilkas, Y. Ishikawa, and U. Kaldor, Chem. Phys. **311**, 163 (2005).

[54] M. S. Safronova, C. J. Williams, and C. W. Clark, Phys. Rev. A **67**, 040303(R) (2003).

[55] M. S. Safronova, C. J. Williams, and C. W. Clark, Phys. Rev. A **69**, 022509 (2004).

[56] S. B. Bayram, M. D. Havey, M. S. Safronova, and A. Sieradzan, J. Phys. B **39**, 2545 (2006).

[57] B. Arora, M. S. Safronova, and C. W. Clark, Phys. Rev. A **76**, 052509 (2007).

[58] B. Arora, M. S. Safronova, and C. W. Clark, Phys. Rev. A **76**, 052516 (2007).

[59] M. S. Safronova, D. Jiang, and U. I. Safronova, Phys. Rev. A **82**, 022510 (2010).

[60] B. Arora, M. S. Safronova, and C. W. Clark, Phys. Rev. A **82**, 022509 (2010).

[61] W. R. Johnson, U. I. Safronova, A. Derevianko, and M. S. Safronova, Phys. Rev. A **77**, 022510 (2008).

[62] W. R. Johnson, S. A. Blundell, and J. Sapirstein, Phys. Rev. A **37**, 307 (1988).

[63] Yu. Ralchenko, F.-C. Jou, D. E. Kelleher, A. E. Kramida, A. Musgrove, J. Reader, W. L. Wiese, and K. Olsen, *NIST Atomic Spectra Database* (version 3.0.2) [http://physics.nist.gov/asd3] (National Institute of Standards and Technology, Gaithersburg, MD, 2006).

[64] L. W. Fullerton and G. A. Rinker, Jr., Phys. Rev. A **13**, 1283 (1976).

[65] P. J. Mohr, Ann. Phys. (NY) **88**, 26 (1974).

[66] P. J. Mohr, Ann. Phys. (NY) **88**, 52 (1974).

[67] P. J. Mohr, Phys. Rev. Lett. **34**, 1050 (1975).

[68] M. S. Safronova, W. R. Johnson, and U. I. Safronova, Phys. Rev. A **53**, 4036 (1996).

[69] M. S. Safronova, W. R. Johnson, and U. I. Safronova, J. Phys. B **30**, 2375 (1997).

[70] W. R. Johnson, Z. W. Liu, and J. Sapirstein, At. Data Nucl. Data Tables **64**, 279 (1996).

[71] M. S. Safronova, W. R. Johnson, and A. Derevianko, Phys. Rev. A **60**, 4476 (1999).
[72] A. Derevianko and E. D. Emmons, Phys. Rev. A **66**, 012503 (2002).
[73] M. S. Safronova and U. I. Safronova, Phys. Rev. A **83**, 012503 (2011).
[74] D. Jiang, B. Arora, and M. S. Safronova, Phys. Rev. A **78**, 022514 (2008).
[75] B. Arora, M. S. Safronova, and C. W. Clark, Phys. Rev. A **76**, 064501 (2007).
[76] M. S. Safronova and W. R. Johnson, Adv. At. Mol. Opt. Phys. **55**, 191 (2007).
[77] J. Mitroy and M. S. Safronova, Phys. Rev. A **79**, 012513 (2009).
[78] D. Jiang, B. Arora, M. S. Safronova, and C. W. Clark, J. Phys. B **42**, 154020 (2009).
[79] E. Iskrenova-Tchoukova and M. S. Safronova, Phys. Rev. A **78**, 012508 (2008).
[80] U. I. Safronova, Phys. Rev. A **82**, 022504 (2010).
[81] U. I. Safronova, Phys. Rev. A **81**, 052506 (2010).
[82] A. Kreuter *et al.*, Phys. Rev. A **71**, 032504 (2005).
[83] U. I. Safronova, M. S. Safronova, and W. R. Johnson, Phys. Rev. A **71**, 052506 (2005).
[84] U. I. Safronova and M. S. Safronova, Phys. Rev. A **78**, 052504 (2008).
[85] W. R. Johnson, D. Kolb, and K.-N. Huang, At. Data Nucl. Data Tables **28**, 333 (1983).
[86] W. R. Johnson, D. R. Plante, and J. Sapirstein, Adv. At. Mol. Opt. Phys. **35**, 255 (1995).
[87] [http://www.webelements.com].
[88] P. Raghavan, At. Data Nucl. Data Tables **42**, 189 (1989).